ChemComm

Aggregation of P3HT as a preferred pathway for its chemical doping by F4-TCNQ

Journal:	*ChemComm*
Manuscript ID	CC-COM-07-2018-005472.R1
Article Type:	Communication

Journal Name

COMMUNICATION

Aggregation of P3HT as a preferred pathway for its chemical doping by F_4-TCNQ

Received 00th January 20xx,
Accepted 00th January 20xx

DOI: 10.1039/x0xx00000x

www.rsc.org/

Kan Tang,[a] Frederick M. McFarland,[a] Skye Travis,[a] Jasmine Lim[b], Jason Azoulay[b], and Song Guo[a]

The chemical doping reaction of P3HT by F_4-TCNQ is studied by optical absorption spectroscopy, atomic force microscopy, and kelvin probe force microscopy. We demonstrate that the P3HT aggregation step is highly preferred before the actual charge transfer step takes place, emphasizing the impacts of morphology on chemical doping reaction of conjugated polymers at molecular level.

Recent years have witnessed an ascending research attention on organic electronics based on conjugated polymers due to its potential advantages in flexibility, cost and processing convenience compared to traditional inorganic materials.[1] Despite the ongoing development of organic electronic materials, their electrical properties such as charge mobilities still lag behind inorganic materials such as crystalline silicon. Thus, chemical doping is brought into practice to improve the electronic performance of conjugated polymers. For example, the electrical conductivity of poly(3-hexylthiophene) (P3HT) is several orders of magnitude higher after being p-doped with 7,7,8,8-tetracyano-2,3,5,6-tetrafluoroquinodimethane (F_4-TCNQ).[2] Among all the chemical doing methods, solution doping is widely applied for conjugated polymer due to its compatibility for various large-scale printing and spraying techniques. [3]

In general, P3HT adopts two basic morphological forms in solution, solubilized form (s-P3HT) and aggregated nanowhisker form (nw-P3HT) that can adopt H-type or J-type aggregation form based on sample preparation conditions.[4] The aggregation process in solution, or the conversion of s-P3HT to nw-P3HT, is typically solubility-driven. Our previous study revealed a clear dependence of P3HT/F_4-TCNQ p-doping reaction kinetics on the morphological forms of P3HT.[5] The doping reaction rate constant of nw-P3HT is about 1000 times larger than that of s-P3HT likely due to promoted initial charge transfer and/or the quick charge delocalization immediately following the charge transfer step. One question remains to be addressed for this doping reaction is that there are two possible mechanisms for the p-doping reaction of s-P3HT by F_4-TCNQ that could lead to same final doping products of $P3HT^+$ and F_4-$TCNQ^-$, as shown in Figure 1. In Mechanism I, fully solubilized s-P3HT undergoes an initial charge transfer (C.T.) with F_4-TCNQ, then the bound ion pair is separated in the charge separation step. In this mechanism, either step can be the rate determining step (R.D.S.). In Mechanism II, the s-P3HT will first aggregate into nw-P3HT, which will then react with F_4-TCNQ. In Mechanism II the first aggregation step will likely be the R.D.S. because our previous studies have demonstrated the quick reaction kinetics between nw-P3HT and F_4-TCNQ.[5]

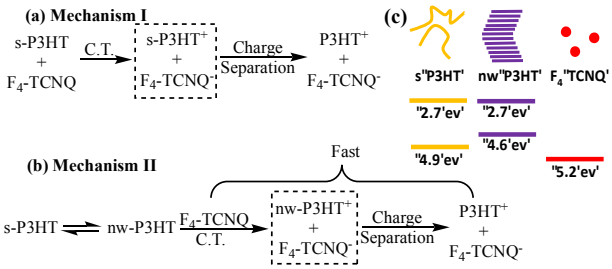

Figure 1. (a-b) Possible reaction pathways for p-doping reaction of s-P3HT by F_4-TCNQ. (c) HOMO and LUMO levels of the s-P3HT, nw-P3HT, and F_4-TCNQ, values are adopted from references.[6]

For the P3HT used in our previous studies (Mn = 70.5 kDa), elevated temperature such as 90°C is required to fully dissolve a moderate concentration (> 0.1 mg/mL) of it in a marginal solvent such as toluene. After cooled down to room temperature, fully solubilized s-P3HT chains would start aggregating into nw-P3HT through π–π stacking between polythiophene segments. This aging process results in the coexistence of s-P3HT and nw-P3HT in P3HT solution at room temperature. However, we have shown that the doping reaction by F_4-TCNQ would simultaneously induce the formation of P3HT aggregates in toluene,[7] which means the final doping product $P3HT^+$ would almost always adopt the aggregated form. So it would be difficult to distinguish the two

[a] Department of Chemistry and Biochemistry, University of Southern Mississippi, Hattiesburg, Mississippi 39406, United States
[b] School of Polymer Science and Engineering, University of Southern Mississippi, Hattiesburg, Mississippi 39406, United States

Electronic Supplementary Information (ESI) available: [details of any supplementary information available should be included here]. See DOI: 10.1039/x0xx00000x

mechanisms listed in Figure 1 unless the formation of nw-P3HT can be excluded with the addition of F_4-TCNQ.

To properly elucidate the mechanism of P3HT p-doped by F_4-TCNQ, herein a low molecular weight (LMW) P3HT (Mw=31.3 kDa) is used. This LMW-P3HT has better solubility in toluene, so within a reasonable concentration range (0.03 – 1 mg/mL), its toluene solution is free of nw-P3HT components (or at least below the detecting limit of optical absorption spectroscopy). In order to induce the aggregation of LMW-P3HT, a poor solvent, such as decane, needs to be added. This anti-solvent addition method is one of the most common crystallization techniques for the formation of conjugated polymer nanostructures in solution.[8] By controlling the exact morphological form of P3HT in solution, we will elucidate the reaction pathway for s-P3HT p-doped with F_4-TCNQ. In addition, the aggregation of LMW-P3HT can also occur during the drying process on a substrate. Atomic force microscopy (AFM) and kelvin probe force microscopy (KPFM) are used to characterize the LMW-P3HT film before and after doping by F_4-TCNQ to provide a microscopic understanding on the morphology-electronic property relationship of P3HT film.

The UV-vis spectra of a LMW-P3HT in toluene (167 µg/mL) is shown in Figure S1. There is only one major absorption peak at 450 nm, which is the π–π* transition peak of s-P3HT in solution.[9] After aging of 24 h the polymer remains exclusively in s-P3HT state. Upon the addition of F_4-TCNQ dopant and sequent 24 h aging, no emergence of characteristic absorbance peaks attributed to either P3HT aggregates (565 nm and 615 nm) or doping products (768 nm and 850 nm) could be observed, shown as the red spectra in Figure 2(a). This result shows that s-P3HT will not undergo noticeable integer charge transfer (ICT) reaction with F_4-TCNQ when remaining in s-P3HT state, which means the Mechanism I proposed in Figure 1 is likely invalid. When 45% decane was added into the freshly prepared LMW-P3HT toluene solution, absorbance peaks centered at 615nm and 565nm formed immediately (shown as the blue spectra in Figure 2(a)), which are attributed to 0–0 and 0–1 vibronic transitions of π–π stacked P3HT aggregates.[9] Interestingly, when 45% decane was added into the freshly prepared LMW-P3HT toluene solution with F_4-TCNQ (similar to the no-doping reaction sample shown as the red spectra in Figure 2(a)), there are immediate emergence of aggregation peaks (565 nm and 615 nm) and absorbance bands centered at 768 nm and 850 nm that can be assigned to the doping products of P3HT polaron/bipolaron and F_4-TCNQ anion, as shown by the green spectra in Figure 2(a). This result indicates that once the P3HT form aggregates, the resulting nw-P3HT will undergo a quick ICT with F_4-TCNQ to generate the doping products, consistent with the Mechanism II. Furthermore, compared with toluene (ε = 2.38), decane (ε = 2.00) is even less non-polar, so this observed anti-solvent induced doping phenomenon probably does not have a charge-transfer step as its R.D.S., which is inconsistent with Mechanism I.

To further consolidate the priority of aggregation on this doping reaction, pre-aggregated P3HT in a 45% decane in toluene was also investigated (Figure 2 (b)). After aging for 6h without dopant in 45% decane, significant amount of aggregation had been developed in LMW P3HT solution, indicating that 45% decane in toluene could be regarded as a rather poor binary solvent for LMW P3HT. Upon the addition of F_4-TCNQ, doping products immediately formed, indicated by the formation of 768 nm and 850 nm peaks. On the contrast, there was absence of aggregation formation for the LMW P3HT in 25% decane case even after 48h of aging. In turn, there was no immediate proceeding of ICT doping reactions when F_4-TCNQ is added because no P3HT aggregates were presented in solution.

In summary, this observation confirmed that aggregation of P3HT is a prerequisite of doping by F_4-TCNQ, which is consistent with Mechanism II. This means that for the reaction pathway in Mechanism I, either the initial C.T. step or the following charge separation step has a large activation barrier that prevents the reaction from taking place. After converting s-P3HT to nw-P3HT, either the redox potential of P3HT is lower to provide more overall driving force or the charge injection/charge delocalization can be promoted because the nw-P3HT has more efficient charge transport characteristics.[6b, 10] Both factors could potentially lower the activation energy of the reaction. So, in the case of pre-aggregated nw-P3HT, its charge transfer reaction with F_4-TCNQ can proceed readily.

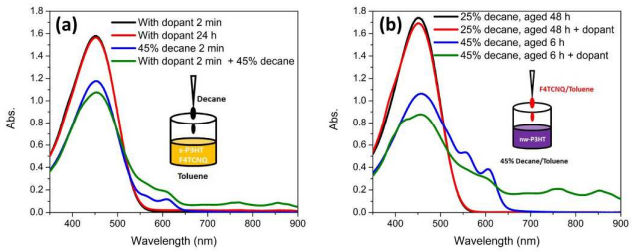

Figure 2. UV-vis spectra of LMW-P3HT solutions (167 µg/mL). 3.7 wt% F_4-TCNQ is added in any doping scenario. (a) Black and red solid lines are for LMW-P3HT in toluene after adding F_4-TCNQ for 2 min and 24 h, respectively. Blue and green solid lines are for LMW-P3HT in toluene with and without F_4-TCNQ after adding 45% decane for 2 min, respectively. (b) Black solid line is for LMW-P3HT in a binary solvent (25% decane in toluene) after aging for 48 h. The UV-vis spectra of the same solution immediately after adding F_4-TCNQ dopant is shown as the red solid line. Blue solid line is LMW-P3HT in a 45% decane in toluene after aging for 6 h. Green solid line is the spectra of the same aged sample immediately after adding F_4-TCNQ dopant. Inset: Schematic drawings on the scenarios in which doping occur are presented.

Despite the confirmation on the priority of aggregation, it would still be worthwhile to elucidate the effect of aging on the doping products because aging is an important measure to manipulate the electronic properties of processed conjugated polymeric materials. Therefore, aging scenarios on doped LMW P3HT in 45% decane in toluene was also investigated with both the dopant and anti-solvent added before any aging or doping starts. In Figure 3, even when there was no dopant presented, absorbance peaks at 615nm and 565nm emerged shortly after the addition of P3HT into binary solvent mixture. The absorbance intensities of these aggregation vibronic peaks increased by at least three folds after 6h, indicating a further development of P3HT aggregates. When dopant F_4-TCNQ is added to the P3HT in 45% decane before the aging process starts, doping reaction immediately occurred because the P3HT molecules readily aggregate into nw-P3HT form. Interestingly, the absorbance bands of doping products

centred at 768 and 850 nm remained unchanged after 2 minutes of doping reaction, indicating the fast kinetics of doping reaction on aggregated P3HT in poor solvent. In another word, doping reaction can be mostly finished within 2 minutes. The intensities of absorbance peaks (565 nm and 615 nm) of P3HT aggregates after 2 minutes of doping were much larger than those in the undoped case after 2 minutes of aging, suggesting a faster initial aggregation rate, which is consistent with our previous report of doping-induced aggregation of P3HT.[4b, 7, 10a, 11] After 6 h of aging, the aggregation absorption intensities are comparable for both cases of with or without the F_4-TCNQ dopant. The slower increase of P3HT aggregates absorption bands after the initial 2 min could be partially due to the conversion of some P3HT aggregates into doping products and the precipitation of P3HT doping products.[2a, 12] Aging scenarios on doped LMW P3HT in 25% and 30% decane in toluene were also examined (Figure S2). Both anti-solvent induced and doping induced aggregation in those cases are much less prominent and slower (~hours) than it in the 45% decane case. Therefore, a new strategy can be developed to control doping rate or morphology of conjugated polymer by fine-tuning of solvent quality and aging.

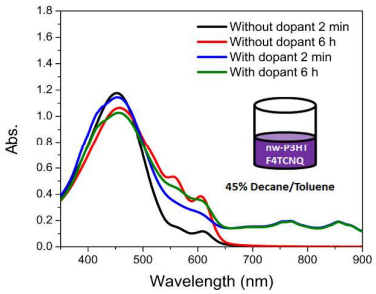

Figure 3 Evolution of UV-Vis spectra of 167μg/mL LMW P3HT in binary solvent (45% decane in toluene) with (blue and olive lines) and without (black and red lines) addition of 3.7wt% F_4-TCNQ dopant. Inset: Schematic drawing on the scenario in which doping occur is presented.

Doping in a solid film by sequential deposition of dopant has attracted ascending research because it provides a promising way of fabricating OSC devices with controlled morphology. In this technique, a suitable orthogonal solvent such as acetonitrile is used so that it only dissolves the dopant but not the host polymer. Film made from this "orthogonal doping" technique shows superior charge transport performance due to well-connected crystalline host polymer domains.[13] Despite some pioneering study on the conductivity of doped P3HT film,[2, 6a, 14] there is still lack of a microscopic understanding on the work function (W) change of conjugated polymer films after "orthogonal doping" by F_4-TCNQ.

Pristine LMW P3HT film is prepared by spin-coating 10 μL of 1 mg/mL P3HT/toluene solution at 2000 rpm for 120 s. This 1 mg/mL P3HT solution is free of detectable aggregates, evidenced by no presence of adsorption peaks attributed to P3HT aggregates (Figure S3). The thickness of the film is determined by AFM measurements (Figure S4) to be about 2.7 nm. F_4-TCNQ was applied to the pristine film using "orthogonal doping" method, i.e. immersed in 225 μg/mL F_4-TCNQ in acetonitrile for 60 s followed by 60 s acetonitrile rinsing to remove the possible leftover F_4-TCNQ. Figure 4 shows the morphological AFM images of pristine P3HT film (a) and doped P3HT film (b). Both of them show characteristics of uniform thin film with surface roughness Ra ~0.5 nm although the thickness of the doped film is increased to 3.7 nm. This is consistent with previous studies showing that "orthogonal doping" does not alter the morphology of the host polymer films.[13] To probe the electronic properties of the films with and without doping, micro-scratches were deliberately made on both films by indentation of an AFM tip. The features of two scratches in Figure 4(a) and (b) are similar and the resulting height profiles are shown in Figure 4(e) exhibiting the same extent of penetration into the films with a depth of about 4 nm. Since the penetration depth is larger than the film thickness, it can be concluded that those two "scratches" can be regarded as exposed ITO substrate.

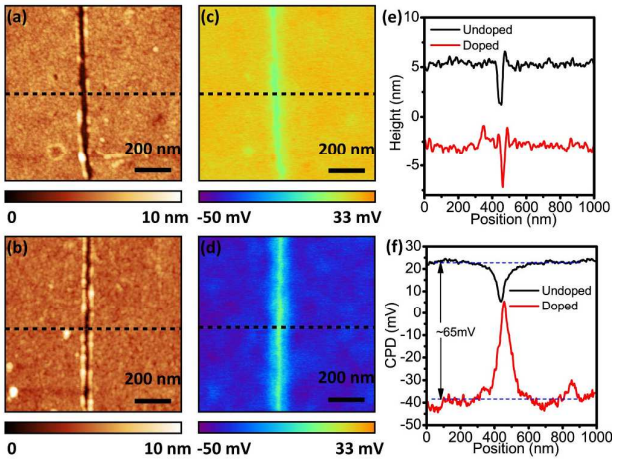

Figure 4. AFM-KPFM results on solid P3HT films prepared from spin-coating 1 mg/ml LMW P3HT in toluene on ITO substrate with and without subsequent doping in 225 μg/mL F_4-TCNQ acetonitrile solution. Scratch was deliberately made on each film by an AFM tip to expose an ITO slit for sequential height and contact potential difference measurements in semicontact mode. The height profiles of two scratches marked in panel (a) and (b) are shown in panel (e), exhibiting similar penetration depth of about 4nm. However, contact potential difference (CPD) of undoped film and doped film (d) show significant difference referring to the exposed ITO substrate. Panel (f) shows the CPD profiles of both undoped and doped P3HT film as marked in panel (c) and (d). Height profiles were vertically shifted for reading convenience while CPD profiles were not shifted.

In KPFM measurements, an abrupt "dip" in contact potential difference (CPD) can be clearly observed due to the exposure of ITO substrate in undoped P3HT film as shown in Figure 4(c). The CPD of undoped P3HT film is about 15 mV higher than that of exposed ITO, which results in the dramatic dip in the CPD profile displayed in Figure 4(f). After orthogonal doping by F_4-TCNQ, the CPD of doped P3HT film appear to be relatively homogeneous at microscopic scale, as shown in Figure 4(d). This is opposite to isolated dopant sites observed in solution mixed doping samples by conductive AFM.[14] The CPD profile of the doped film in Figure 4(f) shows that the CPD of the doped film is about 50 mV lower than the exposed ITO. This means that the work function of doped P3HT film

increases by about 65 mV compared to undoped film, indicating that its Fermi level is mainly decreased by the lowering of HOMO level of the doped film. In addition, the surface dipole induced by F atoms in F_4-TCNQ might also increase the work function of the doped film. The presence of 0-0 and 0-1 vibronic peaks of undoped film in UV-vis (Figure S3) confirms the formation of aggregated LMW P3HT from s-P3HT in solution during the drying process of the film. After dipping this pre-aggregated film into a 225 ug/mL F_4-TCNQ solution, the absorption bands of P3HT polaron/bipolaron and F_4-TCNQ anion centred at 768nm and 850 nm appear. Additionally, significant improvement on the conductivity of the P3HT film after sequential doping was demonstrated (Table S1). The measured conductivity of doped film is about 0.1 S/cm, which is higher than undoped one (~10^{-6} S/cm) by an order of 10^5. This example demonstrates the effectiveness of sequential doping on pre-aggregated P3HT film by transforming P3HT aggregates into P3HT polarons. This approach apparently follows Mechanism II in Figure 1. Herein we have shown films derived from fully solubilized P3HT can undergo aggregation during drying process, which leads to effective doping upon exposure to orthogonal solvent containing dopant molecules.

In conclusion, regioregular LMW-P3HT was used as a model conjugated polymer in a systematic investigation to elucidate the sequence of aggregation and charge transfer in the doping reaction between P3HT and F_4-TCNQ. By excluding possible P3HT aggregation via spontaneous self-assembly and dopant-induced aggregation, we have showed that doping of LMW-P3HT immediately occurs after introducing of an anti-solvent, decane, into a dopant containing P3HT toluene solution. Thus, P3HT aggregation should be regarded as a preferred step for its doping reaction by F_4-TCNQ, which is consistent with the Mechanism II in Figure 1. This result was further strengthened by a control experiment on the comparison between pre-aggregated and aggregation free P3HT solutions. By altering antisolvent/solvent ratio, the time scales on accomplishing doping reaction can be easily tuned between minutes and hours. Fully solubilized P3HT can be transformed into aggregated form in a film after drying. The sequential doping of pre-aggregated film leads to little change on the morphology of the film, but a higher work function of doped P3HT film. We hope the results presented here would resolve the real contribution of aggregated P3HT form on its doping reaction, and be used in the rational and insightful planning of doping process of conjugated polymer in the applications of organic electronics.

This work is supported by a National Science Foundation CAREER award (NSF DMR-1554841). F.M.M. acknowledges the traineeship support from NSF-NRT:INTERFCE (NSF award # 1449999).

Notes and references

1 (a) B. Lüssem; C. M. Keum; D. Kasemann; B. Naab; Z. Bao; K. Leo, *Chem. Rev.*, 2016, **116**, 13714; (b) T. Sekitani; U. Zschieschang; H. Klauk; T. Someya, *Nat. Mater.*, 2010, **9**, 1015; (c) K. Walzer; B. Männig; M. Pfeiffer; K. Leo, *Chem. Rev.*, 2007, **107**, 1233; (d) G. H. Gelinck; H. E. A. Huitema; E. V. Veenendaal; E. Cantatore; L. Schrijnemakers; J. B. P. H. Van Der Putten; T. C. T. Geuns; M. Beenhakkers; J. B. Giesbers; B. H. Huisman; E. J. Meijer; E. M. Benito; F. J. Touwslager; A. W. Marsman; B. J. E. Van Rens; D. M. De Leeuw, *Nat. Mater.*, 2004, **3**, 106.

2 (a) D. T. Scholes; S. A. Hawks; P. Y. Yee; H. Wu; J. R. Lindemuth; S. H. Tolbert; B. J. Schwartz, *J. Phys. Chem. Lett.*, 2015, **6**, 4786; (b) E. F. Aziz; A. Vollmer; S. Eisebitt; W. Eberhardt; P. Pingel; D. Neher; N. Koch, *Adv. Mater.*, 2007, **19**, 3257.

3 (a) G. Wang; W. Huang; N. D. Eastham; S. Fabiano; E. F. Manley; L. Zeng; B. Wang; X. Zhang; Z. Chen; R. Li; R. P. H. Chang; L. X. Chen; M. J. Bedzyk; F. S. Melkonyan; A. Facchetti; T. J. Marks, *Proc. Natl. Acad. Sci.*, 2017, **114**, E10066; (b) Y. Xu; C. Liu; D. Khim; Y.-Y. Noh, *Phys. Chem. Chem. Phys.*, 2015, **17**, 26553; (c) K. J. Baeg; D. Khim; D. Y. Kim; S. W. Jung; J. B. Koo; I. K. You; H. Yan; A. Facchetti; Y. Y. Noh, *J. Polym. Sci., Part B: Polym. Phys.*, 2011, **49**, 62; (d) M. M. Voigt; A. Cuite; D. Y. Chung; R. U. A. Khan; A. J. Campbell; D. D. C. Bradley; F. Meng; J. H. G. Steinke; S. Tierney; L. McCulloch; H. Penxten; L. Luisen; O. Douheret; J. Manca; U. Brokmann; K. Sönnichsen; D. Hülsenberg; W. Bock; C. Barron; N. Blanckaert; S. Springer; J. Grupp; A. McSley, *Adv. Funct. Mater.*, 2010, **20**, 239; (e) H. Yan; Z. Chen; Y. Zheng; C. Newman; J. R. Quinn; F. Dötz; M. Kastler; A. Facchetti, *Nature*, 2009, **457**, 679.

4 (a) F. M. McFarland; B. Brickson; S. Guo, *Macromolecules*, 2015, **48**, 3049; (b) J. Gao; B. W. Stein; A. K. Thomas; J. A. Garcia; J. Yang; M. L. Kirk; J. K. Grey, *J. Phys. Chem. C*, 2015, **119**, 16396.

5 F. M. McFarland; L. R. Bonnette; E. A. Acres; S. Guo, *J. Mater. Chem. C*, 2017, **5**, 5764.

6 (a) H. Méndez; G. Heimel; S. Winkler; J. Frisch; A. Opitz; K. Sauer; B. Wegner; M. Oehzelt; C. Röthel; S. Duhm; D. Többens; N. Koch; I. Salzmann, *Nat. Comm.*, 2015, **6**, 1; (b) W. C. Tsoi; S. J. Spencer; L. Yang; A. M. Ballantyne; P. G. Nicholson; A. Turnbull; A. G. Shard; C. E. Murphy; D. D. Bradley; J. Nelson, *Macromolecules*, 2011, **44**, 2944.

7 F. M. McFarland; C. M. Ellis; S. Guo, *J. Phys. Chem. C*, 2017, **121**, 4740.

8 (a) G. M. Newbloom; P. de la Iglesia; L. D. Pozzo, *Soft Matter*, 2014, **10**, 8945; (b) M. Chang; D. Choi; B. Fu; E. Reichmanis, *ACS Nano*, 2013, **7**, 5402; (c) J. Y. Oh; M. Shin; T. I. Lee; W. S. Jang; Y. Min; J. M. Myoung; H. K. Baik; U. Jeong, *Macromolecules*, 2012, **45**, 7504; (d) W. Xu; L. Li; H. Tang; H. Li; X. Zhao; X. Yang, *J. Phys. Chem. B*, 2011, **115**, 6412; (e) M. He; L. Zhao; J. Wang; W. Han; Y. Yang; F. Qiu; Z. Lin, *ACS Nano*, 2010, **4**, 3241; (f) S. Samitsu; T. Shimomura; S. Heike; T. Hashizume; K. Ito, *Macromolecules*, 2008, **41**, 8000; (g) N. Kiriy; E. Jähne; H. J. Adler; M. Schneider; A. Kiriy; G. Gorodyska; S. Minko; D. Jehnichen; P. Simon; A. A. Fokin; M. Stamm, *Nano Lett.*, 2003, **3**, 707.

9 (a) C. Wang; D. T. Duong; K. Vandewal; J. Rivnay; A. Salleo, *Phys. Rev. B*, 2015, **91**, 085205; (b) J. Clark; C. Silva; R. H. Friend; F. C. Spano, *Phys. Rev. Lett.*, 2007, **98**, 296406; (c) P. J. Brown; D. S. Thomas; A. Köhler; J. S. Wilson; J. S. Kim; C. M. Ramsdale; H. Sirringhaus; R. H. Friend, *Phys. Rev. B*, 2003, **67**, 064203.

10 (a) J. Gao; E. T. Niles; J. K. Grey, *J. Phys. Chem. Lett.*, 2013, **4**, 2953; (b) D. T. Duong; C. Wang; E. Antono; M. F. Toney; A. Salleo, *Org. Electron.*, 2013, **14**, 1330; (c) T. J. Savenije; J. E. Kroeze; X. Yang; J. Loos, *Thin Solid Films*, 2006, **511**, 2; (d) M. Skompska; A. Szkurłat, *Electrochim. Acta*, 2001, **46**, 4007.

11 A. K. Thomas; R. Johnson; B. W. Stein; M. L. Kirk; H. Guo; J. K. Grey, *J. Phys. Chem. C*, 2017, **121**, 23817.

12 (a) J. E. Cochran; M. J. N. Junk; A. M. Glaudell; P. L. Miller; J. S. Cowart; M. F. Toney; C. J. Hawker; B. F. Chmelka; M. L. Chabinyc, *Macromolecules*, 2014, **47**, 6836; (b) J. Gao; J. D. Roehling; Y. Li; H. Guo; A. J. Moulé; J. K. Grey, *J. Mater. Chem. C*, 2013, **1**, 5638.

13 I. E. Jacobs; E. W. Aasen; J. L. Oliveira; T. N. Fonseca; J. D. Roehling; J. Li; G. Zhang; M. P. Augustine; M. Mascal; A. J. Moulé, *J. Mater. Chem. C*, 2016, **4**, 3454.

14 D. T. Duong; H. Phan; D. Hanifi; P. S. Jo; T. Q. Nguyen; A. Salleo, *Adv. Mater.*, 2014, **26**, 6069.

Conflicts of interest

There are no conflicts to declare.

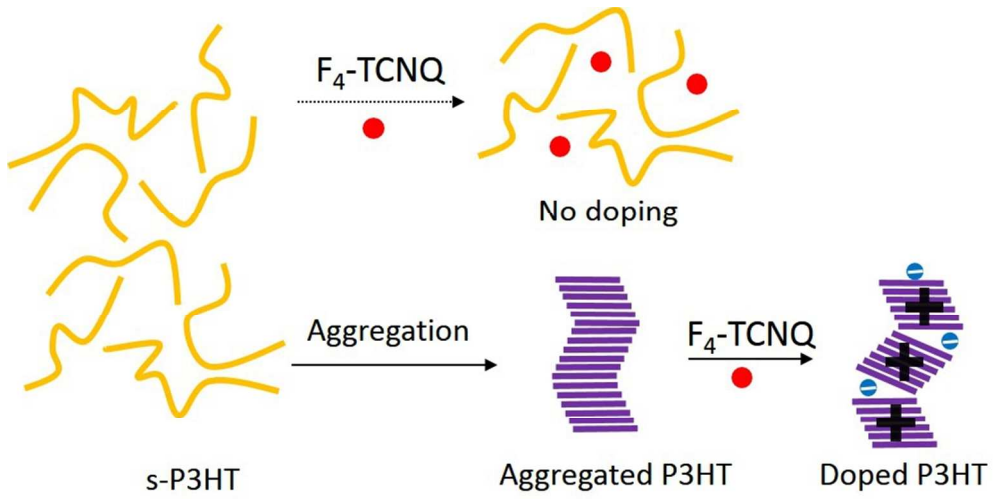

265x135mm (96 x 96 DPI)